On Hybrid Approach in Microwave Scattering Theory for Wire-filled Composites

Azim Uddin[1], **Yujie Zhao**[2], **and Faxiang Qin**[1]

[1]Institute for Composites Science Innovation (InCSI), School of Materials Science & Engineering
Zhejiang University, 38 Zheda Road, Hangzhou 310027, China
[2]School of Physics and Astronomy, University of St. Andrews, Fife KY16 9SS, Scotland

2021 Photonics & Electromagnetics Research Symposium (PIERS) | 978-1-7281-7247-7/21/$31.00 ©2021 IEEE | DOI: 10.1109/PIERS53385.2021.9694931

Abstract— A hybrid approach to the scattering theory in composite materials with conductive wire inclusions has been discussed that allows considering their material properties such as conductivity and magnetic domain structure. The wire geometry of the inclusions makes it possible to determine a unique parameter — the surface impedance, which can be accurately measured over a wide frequency range, from kilohertz to tens of gigahertz. The surface impedance includes both conductive and magnetic properties of wires that determine their microwave scattering properties. The scattered EM field from a single wire can then be rigorously calculated by solving the integro-differential antenna equation for the linear current density with the impedance boundary condition. The field within the skin-layer in conductive ferromagnetic wires is strongly affected by external stimuli, such as DC magnetic field, tensile stress, and temperature, which open up additional channels to tune the scattered microwave radiation. Within the framework of the proposed hybrid approach, combining metrological measurements of individual properties of wires and accurate solution of an external electrodynamic problem, there is no need to consider the most complex internal problem. The developed approach has been used to calculate the dipole moment induced by an external wave in a short ferromagnetic wire. The surface impedance of the wire in the presence of a longitudinal DC magnetic field and tensile stress was measured in a specially designed PCB cell. The numerical algorithm for solving the antenna equation with the impedance boundary condition was implemented in PyCharm IDE. The single-particle scattering problem is the key stage to constructing a general theory that considers the collective response of many particles, as well as their EM coupling.

1. INTRODUCTION

The electromagnetic (EM) composites with conductive and non-conductive inclusions have been widely studied over the past decades. The early works dealt with optical properties of tiny metallic spheres suspended in a dielectric. Historically first Mie's theory provided a rigorous solution for the diffraction of a plane monochromatic wave by a homogeneous sphere [1, 2]. A variety of established theories and measurement techniques in optics are centred around two main phenomena. Metallic particles can enhance the surface field by several orders of magnitude [3], while dielectric particles, considered as resonate cavities, can have exceptionally high quality factors [4] or focus light into sub-wavelength photonic jets [5].

In the frame of classical field theory, the electrodynamic methods for solving scattering problems are not tied to a specific wavelength and can be used both in the optical and microwave parts of the spectrum. However, the material equations, which must supplement Maxwell's equations, are defined by the frequency range, thus resulting in specific optical or microwave effects. In the microwave (so we will denote the corresponding frequency range), the penetration depth of the EM field within the skin-layer of a metallic particle can be comparable to its characteristic size even for micron dimensions. On the contrary, in optics, the internal structure of a micron metallic particle would be irrelevant due to complete EM shielding. In the microwave, the dielectric polarization anisotropy in small particles will not play any significant role in comparison with the optics. However, in optics, we will not encounter the variety of effects caused by the coupling of magneto-anisotropic and conductive properties observed in the microwave [6]. Therefore, the total EM response depends both on shape and material properties of the particles, with internal and scattered EM fields being solutions of the macroscopic Maxwell's equations that satisfy the appropriate boundary conditions at the surface of the particle and at infinity.

For some media or excitation regimes, the very division into macroscopic Maxwell's equations and supplementing them with material equations may require special consideration. For linear scattering regimes, this division can usually be done. But even in this case, the models describing material properties may not be accurate enough to reproduce the experimental data. In the case of ferromagnetic wires, the conditions under which magnetic anisotropy is formed during the casting

Authorized licensed use limited to: Zhejiang University. Downloaded on February 09,2022 at 03:31:29 UTC from IEEE Xplore. Restrictions apply.

process [7] and the resulting magnetic domain structure [8] are extremely complex. The widely used model [9] for the high frequency field-tunable impedance (so-called magneto-impedance, MI), which combines magnetic and conductive properties, cannot provide a quantitative agreement with experiments. Recently, we put forward an idea of a hybrid approach [10], the essence of which is as follows. The experimentally measured high-frequency impedance can be used as a boundary condition at the wire surface in the integro-differential antenna equation for the current density induced by an external EM wave [11]. Thus, it becomes possible to avoid considering the internal problem and reduce the scattering to a purely electrodynamic problem of radiation from a linear current. The impedance of thin ferromagnetic wires can be precisely measured under external stimuli such as DC magnetic field, tensile stress, or temperature.

The goal of the microwave scattering theory in composite materials with micro/nano inclusions in a polymer matrix is to quantitatively predict reflection and transmission properties. The single-particle scattering problem is the key stage to constructing a general theory that considers the collective response of many particles, as well as their EM coupling. In our present work, we have demonstrated the hybrid approach for numerically solving the antenna equation, supplemented with the experimentally measured surface impedance, for a short ferromagnetic wire. The surface impedance was measured in a specially designed PCB cell that allows applying both a longitudinal DC magnetic field and tensile stress. Scattering from short wire inclusions will be of dipoles in nature, i.e., Lorentzian type of dispersion. Thus, in order to demonstrate the influence of external stimuli, as well as resistive and radiation losses, on scattering, the linear current density in a single wire (found from the antenna equation) was recalculated into the dipole moment. The latter was calculated for a wide frequency range, including antenna and ferromagnetic resonances. As expected, all effects will be enhanced in the vicinity of the antenna resonance. Increasing frequency, the radiation losses also increase, which determine (along with resistive losses) the magnitude of the antenna resonance. On the contrary, the effects associated with the magnetic structure of the wires, including the field and stress tunabilities, significantly wane at a few gigahertz.

The EM properties of composites will play an increasing role in relevant applications. This is especially true for stealth technologies and methods of remote non-destructive testing (NDT) [12]. Ferromagnetic inclusions bring additional sensory functions, thereby expanding the range of potential applications.

2. ANTENNA EQUATION WITH THE IMPEDANCE BOUNDARY CONDITION

In this section, we outline the main concepts used for modelling microwave response from a thin ferromagnetic wire [11]. CGS units are used. A thin wire conductor with the length l (cm) and the radius a (cm), embedded into a medium with ε and μ, is irradiated by a plane wave. The wavelength λ and l are assumed to be much larger than the wire diameter $2a$. The projection of the wave electric field $\bar{e}_{x0}$ onto the wire direction (x-axis) induces a longitudinal current distribution. This current determines the scattered EM field with the longitudinal electric field $\bar{e}_x$ and the circular magnetic field $\bar{h}_\varphi$ on the wire surface. The same field components $(\bar{e}_x, \bar{h}_\varphi)$ can be induced by a current flowing along the wire axis with the volume density $j(x)\delta_s$, where $\delta_s(y,z)$ is two-dimensional Dirac's function. The function $j(x)$ will be further referred to as "linear current". The projection of the wave longitudinal magnetic field $\bar{h}_{x0}$ onto the wire direction induces a circular eddy (in both magnetic or non-magnetic wire). This current determines the scattered EM field with the circular electric field $\bar{e}_\varphi$ and the longitudinal magnetic field $\bar{h}_x$ on the wire surface. The field components $(\bar{e}_\varphi, \bar{h}_x)$ cannot be induced by a linear current. However, due to the tiny wire diameter the contribution of this field to the scattered response will be negligible. For magnetic wires with a certain type of magnetic anisotropy [9, 13], $\bar{h}_{x0}$ may also induce a longitudinal electric field that will contribute to $\bar{e}_x$ induced by $\bar{e}_{x0}$.

The most general form of the boundary conditions on the wire surface can be written though the surface impedance [14]: $\bar{\mathbf{E}}_t = \hat{\varsigma}\,(\bar{\mathbf{H}}_t \times \mathbf{n})$, where $\mathbf{n}$ is the unit normal vector directed inside the conductor, $\bar{\mathbf{E}}_t$ and $\bar{\mathbf{H}}_t$ are the tangential vectors of the total electric and magnetic fields at the wire surface, which include both the scattered and external fields. In the cylindrical coordinate system (x, φ, r), the impedance boundary condition will take the following form:

$$\begin{aligned} \bar{E}_x &= \varsigma_{xx}\bar{H}_\varphi - \varsigma_{x\varphi}\bar{H}_x \\ \bar{E}_\varphi &= \varsigma_{\varphi x}\bar{H}_\varphi - \varsigma_{\varphi\varphi}\bar{H}_x \end{aligned} \tag{1}$$

In a nonmagnetic conductor $\varsigma_{x\varphi} = \varsigma_{\varphi x} \equiv 0$. All surface impedance components can be accurately measured in experiment under different stimuli: DC magnetic field, tensile stress, and temperature.

Authorized licensed use limited to: Zhejiang University. Downloaded on February 09,2022 at 03:31:29 UTC from IEEE Xplore. Restrictions apply.

The circular component $\bar{E}_\varphi$ will give a negligible contribution to the scattered radiation. Using (1), for the total longitudinal electric field we can write:

$$\bar{E}_x = \bar{e}_x + \bar{e}_{0x} = \varsigma_{xx}\bar{h}_\varphi(x) - \varsigma_{x\varphi}\bar{h}_{0x}(x) \tag{2}$$

Expressing $\bar{h}_\varphi(x) = (2/ac)(G_\varphi * j)$ and $\bar{e}_x = -(4\pi/i\,\omega\,\varepsilon)[\partial^2(G*j)/\partial\,x^2 + k^2(G*j)]$ through the corresponding convolutions of the Green's function with $j(x)$, we finally obtain the following integro-differential equation:

$$\frac{\partial^2}{\partial\,x^2}(G*j) + k^2(G*j) = \frac{i\,\omega\,\varepsilon}{4\pi}\bar{e}_{0x}(x) - \frac{i\,\omega\,\varepsilon\,\varsigma_{xx}}{2\,\pi a\,c}(G_\varphi * j) + \frac{i\,\omega\,\varepsilon\,\varsigma_{x\varphi}}{4\pi}\bar{h}_{0x}(x) \tag{3}$$

where i is the imaginary unit, $k = (\omega/c)\sqrt{\varepsilon\,\mu}$ is the wave number, c is the speed of light (cm/s), $G_\varphi(r) = a^2(1 - i\,k\,r)\exp(i\,k\,r)/(2r^3)$, and $G(r) = \exp(i\,k\,r)/(4\,\pi\,r)$.

The convolution over the wire length is defined as $(F*j) = \int\limits_{-l/2}^{l/2} j(s)F(r)ds$, where $F(r)$ is a function of $r = \sqrt{(x-s)^2 + a^2}$. Eq. (3) has to be supplemented with the boundary conditions at the wire ends: $j(-l/2) = j(l/2) \equiv 0$.

The real functions $\mathrm{Re}(G)$ and $\mathrm{Re}(G_\varphi)$ have a sharp peak when $r = a$, and hence they give the main contributions to the convolutions:

$$(\mathrm{Re}(G)*j) \;\approx\; j(x)\int\limits_{-l/2}^{l/2}\mathrm{Re}(G(r))ds = j(x)\,Q \tag{4}$$

$$(\mathrm{Re}(G_\varphi)*j) \;\approx\; j(x)\int\limits_{-l/2}^{l/2}\mathrm{Re}(G_\varphi(r))ds = j(x)Q_\varphi \tag{5}$$

where $Q \sim \ln(l/a)/(2\pi)$ and $Q_\varphi \sim 1$.

The convolutions with the imaginary parts of G and G_φ take into account the radiation losses which may significantly modify the dispersion curves in the vicinity of the antenna resonances. The role of these terms increases with increasing frequency. For nano-inclusions in the optical range, radiation losses can even exceed the resistive ones [15]. Using (4) and (5), we can exclude singularities in the convolution kernels, so that (3) will take the following form:

$$\begin{aligned}&\frac{\partial^2}{\partial\,x^2}\left[j(x) + \frac{i}{Q}(\mathrm{Im}(G)*j)\right] + \tilde{k}^2\left[j(x) + \frac{i}{Q}(\mathrm{Im}(G)*j)\right]\\ &= \frac{i\,\omega\,\varepsilon}{4\pi\,Q}\left[\bar{e}_{0x}(x) + \varsigma_{x\varphi}\bar{h}_{0x}(x)\right] + \frac{i(\tilde{k}^2 - k^2)}{Q}(\mathrm{Im}(G)*j) + \frac{\omega\,\varepsilon\,\varsigma_{xx}}{2\,\pi\,a\,c\,Q}(\mathrm{Im}(G_\varphi)*j)\end{aligned} \tag{6}$$

where $\tilde{k} = \frac{\omega}{c}\sqrt{\varepsilon\mu}(1 + \frac{i\,c\,\varsigma_{xx}}{2\,\pi\,a\,\omega\,\mu Q})^{1/2}$ is the new wavenumber taking into account the impedance boundary condition. Inverting the operator $\partial^2/\partial\,x^2 + \tilde{k}^2$, we obtain a Fredholm integral equation of the second kind with free constants A and B that can be solved by successive iterations [11]. The constants A and B have to be chosen to satisfy the boundary conditions $j(-l/2) = j(l/2) \equiv 0$.

Zero iteration is obtained for $\mathrm{Im}(G) = 0$ and $\mathrm{Im}(G_\varphi) = 0$:

$$j_0(x) = A\sin(\tilde{k}\,x) + B\cos(\tilde{k}\,x) + \frac{i\,\omega\,\varepsilon(\bar{e}_0 + \varsigma_{x\varphi}\bar{h}_0)}{4\,\pi\,Q\,\tilde{k}^2} \tag{7}$$

Satisfying the boundary conditions $j_0(-l/2) = j_0(l/2) \equiv 0$, we obtain:

$$j_{0[-l/2,l/2]}(x) = \frac{i\,\omega\,\varepsilon(\bar{e}_0 + \varsigma_{x\varphi}\bar{h}_0)}{4\pi Q\,\tilde{k}^2} \times \frac{(\cos(\tilde{k}\,l/2) - \cos(\tilde{k}\,x))}{\cos(\tilde{k}\,l/2)} \tag{8}$$

The iterations are continued according to the scheme $j_n = j_0(x) + \hat{\mathbf{A}}j_{n-1}$ starting from (8), where $\hat{\mathbf{A}}$ is the sum of convolution operators obtained after inverting $\partial^2/\partial\,x^2 + \tilde{k}^2$. The constants A and

Authorized licensed use limited to: Zhejiang University. Downloaded on February 09,2022 at 03:31:29 UTC from IEEE Xplore. Restrictions apply.

B have to be chosen when the iterations are finished. In our numerical algorithm written in Python using PyCharm IDE we implemented the zero and first iterations.

Since the scattering in the radiative near/far fields will be of a dipole nature, we recalculated the linear current density to the dipole moment, which will be used for numerical analysis. Using the continuity equation written in the frequency domain, $\partial j(x)/\partial x = i\omega\rho(x)$, we obtain for the dipole moment D:

$$D = \int_{-l/2}^{l/2} \rho(x)dx = \frac{i}{\omega}\int_{-l/2}^{l/2} j(x)dx \tag{9}$$

3. MEASURING THE SURFACE IMPEDANCE IN FERROMAGNETIC WIRES

The surface impedance ς_{xx} can be obtained from the experimentally measured high-frequency impedance Z. For a current Iinduced by a potential difference V across the wire, the circular magnetic field on the wire surface is (CGS units):

$$\bar{H}_\varphi = \frac{2I}{ac} = \frac{2V}{Zac} = \frac{2l\bar{E}_x}{Zac} \tag{10}$$

Since, according (1), $\varsigma_{xx} = \bar{E}_x/\bar{H}_\varphi$, we obtain:

$$\varsigma_{xx}^{\text{cgs}} = \frac{10^9 aZ[\Omega]}{2cl} \tag{11}$$

where the surface impedance in CGS was expressed through the impedance in SI. This parameter includes all information about both conductive and magnetic properties. The second parameter $\varsigma_{x\varphi}$ is more difficult for experimental verification, but it differs from zero only for wires with a specific magnetic anisotropy. We will not consider this case.

The method for wideband measurements of the wire impedance, subjected to the external DC magnetic field and tensile stress, was developed in Ref. [10]. The measurement setup, shown in Fig. 1, includes a 2-port Vector Network Analyser (VNA), stress machine, Helmholtz coil, dog-bone PCB cell, calibration PCB cell with the surface mount SOLT terminations (SHORT, OPEN, LOAD, THRU), and a stress control sensor. The PCB, made of Rogers' material, contains 50 Ω microstrips on one side and a continuous ground plane on the opposite side.

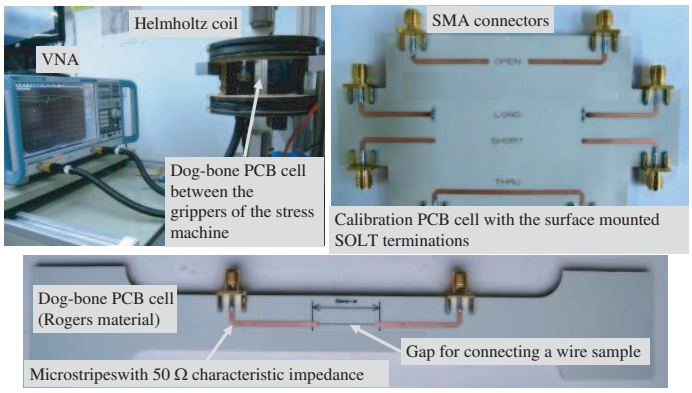

Figure 1: Experimental setup for the broadband measurement of the wire impedance subjected to the external DC magnetic field and tensile stresses.

After the SOLT calibration, the reference plane is shifted to the ends of the wire sample which is placed on the surface of the dog-bone PCB cell. The ends of the wire are glued with the silver paint to the free ends of microstrips. A wire above the ground plane is a waveguide that introduces additional phase distortions that cannot be eliminated by the calibration. To compensate them, we used a phase unwrapping technique.

4. NUMERICAL SIMULATIONS AND DISCUSSIONS

To demonstrate the hybrid approach, we solved (6) with ς_{xx} which was experimentally measured in a Co-based glass-coated ferromagnetic wire of the composition (wt%) $Co_{68.7}Fe_4Si_{11}B_{13}Ni_1Mo_{2.3}$

Authorized licensed use limited to: Zhejiang University. Downloaded on February 09,2022 at 03:31:29 UTC from IEEE Xplore. Restrictions apply.

produced by the Taylor-Ulitovsky method [7]. The current distribution along the wire was calculated up to the first iteration as explained above. The wire sample had a metal core diameter of 18.6 µm, total diameter of 21.6 µm (including the glass shell), and the length of 2.5 cm. During impedance measurements, the wire was subjected to the longitudinal DC bias magnetic field and tensile stress. Fig. 2 demonstrates the transformation of the impedance dispersion in a wide frequency range under bias field and tensile stress.

The impedance becomes stress-sensitive only in the presence of a bias field what is typical for wires with a circumferential anisotropy. For our wire, the highest stress sensitivity was observed in the vicinity of the ferromagnetic resonance 640 MHz at the bias field 5.5 Oe. All effects will be enhanced at the antenna resonance caused by the current distribution along a short wire:

$$\lambda_{res} = 2l\sqrt{\varepsilon\mu}\,\mathrm{Re}\left(1 + \frac{i\,c\,\varsigma_{xx}}{2\,\pi\,a\,\omega\,\mu Q}\right)^{1/2} \tag{12}$$

For numerical calculations, we used ς_{xx} obtained from Z according to (10). The dispersion of dipole moment in Fig. 3, calculated for $j_0(x)$ and $j_1(x)$ (zero and first iteration), demonstrates the importance of taking into account the radiative losses in the vicinity of antenna resonance. Radiative losses associated with the disper1 curves (real and imaginary part) further moderate the resonance magnitude as compared with disper0 (only resistive losses). This effect will only increase if the antenna resonance occurs at higher frequencies.

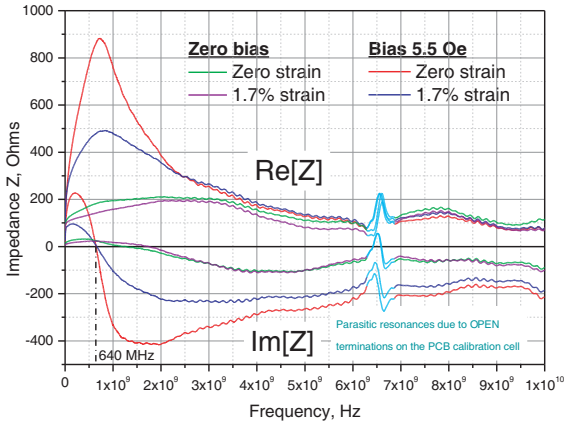

Figure 2: Frequency dispersion of impedance measured in the presence of bias fields (0 or 5 Oe) and tensile strains (0 or 1.7%) [10].

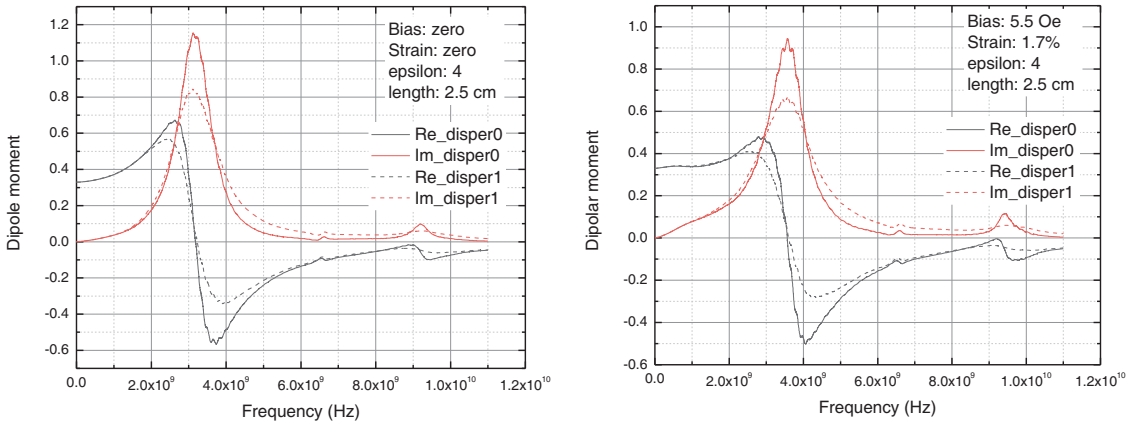

Figure 3: Frequency dispersion of the dipole moment calculated using experimentally measured ς_{xx} for zero (disper0) and first (disper1) iterations of the current distribution at 0–12 GHz.

The strain sensitivity at 4 GHz in the presence of a bias field, see Fig. 3, is already not strong even at the antenna resonance. To reduce the resonance frequency, we increased the wire length (l = 6 cm) and permittivity (ε = 9). Fig. 4 shows the excitation mode when the ferromagnetic

Authorized licensed use limited to: Zhejiang University. Downloaded on February 09,2022 at 03:31:29 UTC from IEEE Xplore. Restrictions apply.

resonance is close to the antenna resonance. The resonance magnitude and its width (quality factor) demonstrate strong field sensitivity. The stress sensitivity also became stronger. At zero bias field the resonance is much narrower because the impedance is lower (see Fig. 2). The effect of radiative losses is now faded what is explained by lower frequencies and prevailing resistive losses.

We have considered the simplest shape for a wire inclusion in the form of a straight dipole. Antenna equation with impedance boundary conditions can be generalized for more complex shapes such as split loops, flat and volumetric spirals.

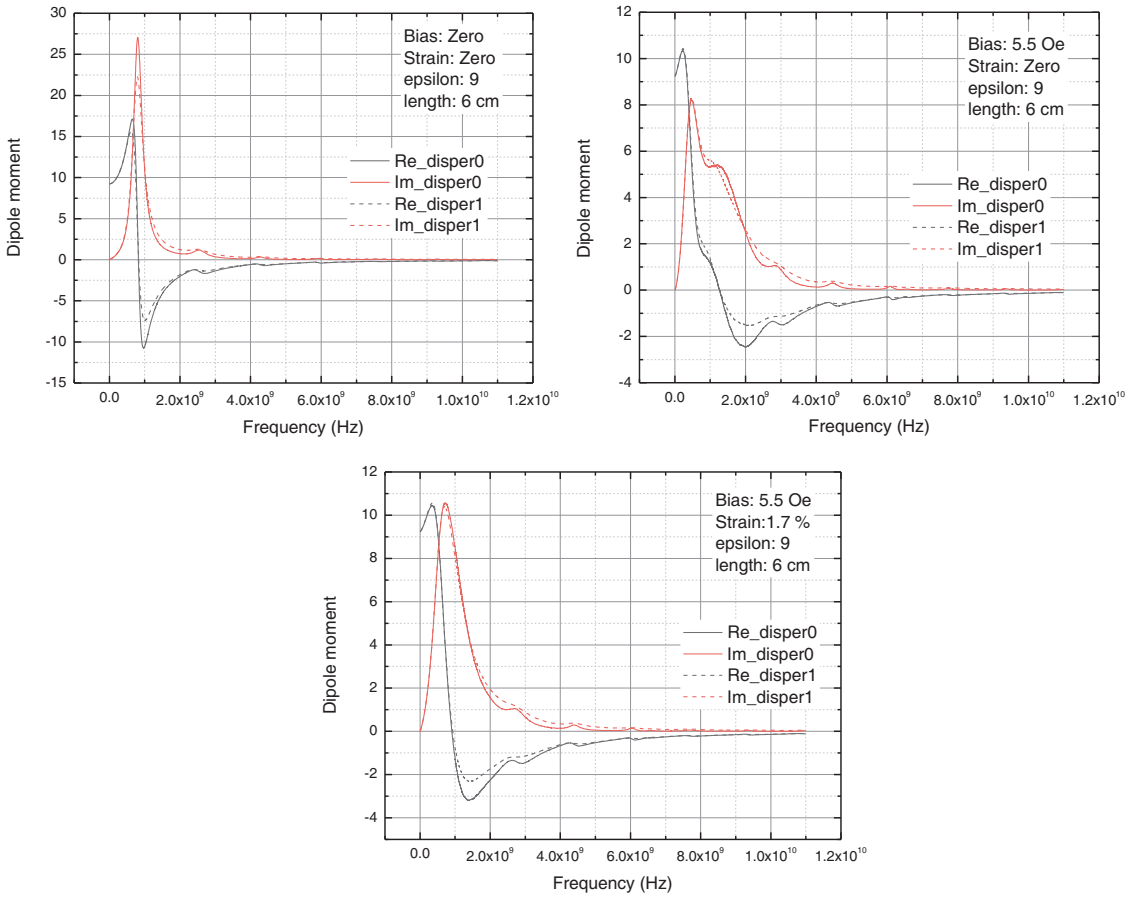

Figure 4: Frequency dispersion of the dipole moment calculated using experimentally measured ς_{xx} when the antenna resonance is close to the ferromagnetic resonance at 0–12 GHz.

5. CONCLUSIONS

Modern algorithms and commercial solvers are able to simulate the distribution of EM fields from objects of complex geometry. To reproduce the EM properties of the constituting materials, it is often possible to get by with standard models that have a small number of adjustable parameters sufficient to describe dispersion and resonance behaviour. However, there are classes of problems that cannot be solved within the framework of this approach. In this work, we have demonstrated a hybrid method for calculating microwave scattering from thin ferromagnetic wires. The proposed approach makes it possible to avoid solving the internal problem, reducing the consideration to only the external electrodynamic problem. Since the high-frequency impedance characteristics of ferromagnetic wires can be accurately measured, it becomes possible to build a practically predictive scattering theory for composite materials containing such wire-shaped inclusions.

ACKNOWLEDGMENT

The authors are grateful to Dr. Dmitriy Makhnovskiy for building a multifunctional microwave laboratory at InCSI (Hangzhou) and discussing the idea of the hybrid approach in the scattering theory for wire-filled composites.

Authorized licensed use limited to: Zhejiang University. Downloaded on February 09,2022 at 03:31:29 UTC from IEEE Xplore. Restrictions apply.

REFERENCES

1. Born, M. and E. Wolf, *Principles of Optics: Electromagnetic Theory of Propagation, Interference and Diffraction of Light*, Elsevier, 2013.
2. Newton, R. G., *Scattering Theory of Waves and Particles*, Springer Science & Business Media, 2013.
3. Hillenbrand, R. and F. Keilmann, "Optical oscillation modes of plasmon particles observed in direct space by phase-contrast near-field microscopy," *Appl. Phys. B*, Vol. 73, 239, 2001.
4. Vahala, K. J., "Optical microcavities," *Nature*, Vol. 424, 839, 2003.
5. Kong, S., et al., "Photonic nanojet-enabled optical data storage," *Optics Express*, Vol. 16, 13713, 2008.
6. Panina, L. V. and K. Mohri, "Magneto-impedance effect in amorphous wires," *Appl. Phys. Lett.*, Vol. 65, 1189, 1994.
7. Larin, V. S., et al., "Preparation and properties of glass-coated microwires," *J. Mag. Magn. Mater.*, Vol. 249, 39, 2002.
8. Jiang, S. D., et al., "Relating surface roughness and magnetic domain structure to giant magneto-impedance of Co-rich melt-extracted microwires," *Sci. Rep.*, Vol. 7, 46253, 2017.
9. Makhnovskiy, D. P., et al., "Field-dependent surface impedance tensor in amorphous wires with two types of magnetic anisotropy: Helical and circumferential," *Phys. Rev. B*, Vol. 63, 144424, 2001.
10. Zhao, Y., et al., "Novel broadband measurement technique on PCB cells for the field-and stress-dependent impedance in ferromagnetic wires," *Meas. Sci. Tech.*, Vol. 31, 025901, 2020.
11. Makhnovskiy, D. and L. Panina, "Field-tunable permittivity of composite materials containing ferromagnetic wires," *J. Appl. Phys.*, Vol. 93, 4120, 2003.
12. Li, Z., et al., "Applications of microwave techniques for aerospace composites," *2017 IEEE International Conference on Microwaves, Antennas, Communications and Electronic Systems (COMCAS)*, 2017.
13. Sandacci, S., et al., "Off-diagonal impedance in amorphous wires and its application to linear magnetic sensors," *IEEE Tran. Magn.*, Vol. 40, 3505, 2004.
14. Landau, L. D. and E. M. Lifshitz, *Electrodynamics of Continuous Media*, Pergamon Press, 1975.
15. Panina, L. V., et al., "Optomagnetic composite medium with conducting nanoelements," *Phys. Rev. B*, Vol. 66, 155411, 2002.

Authorized licensed use limited to: Zhejiang University. Downloaded on February 09,2022 at 03:31:29 UTC from IEEE Xplore. Restrictions apply.